Facile morphology control of gold(0) structures from aurophilic assemblies

Elisabet Aguiló,[a] Mariona Dalmases,[a,b] Mengxi Lin,[a,b] João Carlos Lima,[c] Raquel Gavara,[a] Albert Figuerola,[a,b,*] Jordi Llorca,[d,*] Laura Rodríguez.[a,b,*]

[a] Departament de Química Inorgànica i Orgànica, Secció de Química Inorgànica, Universitat de Barcelona, Martí i Franquès 1–11, 08028 Barcelona (Spain). e-mail: laura.rodriguez@qi.ub.es, albert.figuerola@qi.ub.es

[b] Institut de Nanociència i Nanotecnologia (IN2UB). Universitat de Barcelona, 08028 Barcelona (Spain).

[c] LAQV-REQUIMTE, Departamento de Química, Universidade Nova de Lisboa. Monte de Caparica (Portugal)

[d] Institute of Energy Technologies, Department of Chemical Engineering and Barcelona Research Center for Multiscale Science and Engineering. Universitat Politècnica de Catalunya, EEBE Eduard Maristany 10-14, 08019 Barcelona (Spain). e-mail: jordi.llorca@upc.edu

Abstract

Different gold microstructures have been synthesized by using supramolecular gold(I) organometallic compounds as templates and Ag nanoparticles as reducing agent. The use of fibers resulting from supramolecular assemblies of neutral gold(I) compounds, gives rise to the formation of microrods. The use of supramolecular assemblies from ionic molecules results in spherical or square-based prisms gold microstructures, depending on the shape of the supramolecular gold(I) precursor assembly. In addition to temperature and reaction time, the solvent has a strong influence on the formation and morphology of the gold structures. Well-defined star-like morphologies have been obtained in chloroform.

Keywords: supramolecular assemblies, reduction, Au microstructures, morphology control, Au(I), Ag NPs

There has been a widespread and rapid increasing interest in gold structures owing to their unique physical, chemical, and biocompatible properties, as well as promising applications in different fields such as catalysis, sensing, bioimaging, photothermal therapy, drug delivery, nanoelectronics, and the fabrication of photonic and plasmonic devices.[1–3] A variety of colloidal chemical methods have been developed to fabricate gold nanocrystals with specific shapes, including rods, wires, belts, combs, plates, prisms, polyhedra, cages, frames, caps, stars and flowers, as well as dendrites.[2,4,5]

Positioning or organizing noble metal nanostructures is a key process in the fabrication of plasmonic interfaces with unusual geometries. The design of functional superarchitectures has often been realized by the use of facile templating approaches, where degradable polymers,[6,7] surfactant micelles[8,9] or mesoporous silica, zeolites, and alumina membranes have been used as organized structural scaffolds.[10] These templates dictate the shape and ease the formation of ordered porous nanostructures and other types of architectures, while either pre-made or in-situ synthesized noble metal nanoparticles are used as building blocks, delivering the desired functional plasmonic properties pursued. Thus, a sufficiently strong interaction between the templating surface and the noble metal nanoparticles (or the noble metal molecular precursor) is mandatory in order to guarantee a quantitative coverage of the template surface and the efficient transfer of the template geometry into the noble metal-based superstructure. The enhancement of such interaction might require additional functionalization steps or it might limit the combination of the templating agent and the noble metal precursors used depending on their chemical affinity.[11–14]

Organometallic Au(I) compounds are a class of fluorescent molecules with a boundless variety of molecular structures and functionalization groups.[15,16] The establishing of weak intermolecular interactions in solution is responsible for the formation of supramolecular structures based on H bonds, π-π stacking and aurophilic interactions among others.[17] Thus, tailoring their organic skeleton becomes a key aspect for controlling size and shape of the supramolecular assembly obtained. Additionally, the presence of Au(I) atoms in the structure converts this templating or structure-directing agent into a ready-to-react precursor of the plasmonic superstructure. In this way, the noble metal precursor is already incorporated in the template and no further interaction needs to be enhanced with a building block in a second step. Thus, the direct application of an external stimuli like heat, electron beam or other types of reducing agents[18] an be

enough for obtaining the plasmonic architectures pursued, in which the geometry of the previous supramolecular assembly has been transferred. A similar approach has been recently exploited by Ezquerra *et al.*, who demonstrated the feasibility of thermal processing routes to form good quality molecular junctions from organometallic assemblies of relatively complex molecular structure capped with uniformly-shaped Au nanoparticles formed *in situ*.[19]

We previously demonstrated the formation of long hollow fibers in aqueous solutions of neutral gold organometallic compounds[20–25] due to the establishment of aurophilic and other type of weak contacts, which are particularly favored in polar solvents.[26,27] Additionally, we observed that modulation of the chemical structure mainly by methylating (by obtaining ionic species) and additionally varying the counterion gives rise to the formation of different shapes, from fibers (neutral compounds) to vesicles (methylated derivative containing iodine as counterion) or squares (methylated compound containing triflate as counterion).[28] On the other hand, we also reported the reduction of gold(I) organometallic supramolecular assemblies to well-controlled Au(0) nanoparticles with different sizes upon irradiation of light, electrons or temperature.[21] The combination of inter- and intramolecular electrostatic and Au(I)···Au(I) aurophilic and other type of weak interactions define the path for the alignment of the assemblies and constitutes the driving force for the morphological transformation under certain conditions[29–32]. But, besides nanoparticle or nanocluster formation, it has been reported in the literature that the presence of aurophilic contacts between AuCl(oleylamine) molecules can also induce the formation of very thin nanowires when the reduction is performed by using silver NPs.[29] This methodology, although very promising, has not been widely explored.

In this work, we use organometallic units (A, B, C in Chart 1) that present different supramolecular morphologies when they self-assemble (D, E, F in Chart 1) as a template to obtain different types of well-defined Au(0) architectures with different shapes, by using silver NPs as reducing agent. The supramolecular shapes of the organometallic assemblies determines the resulting Au(0) microshapes.

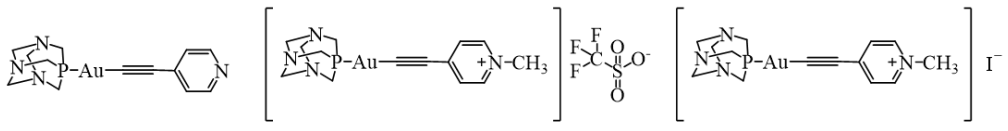

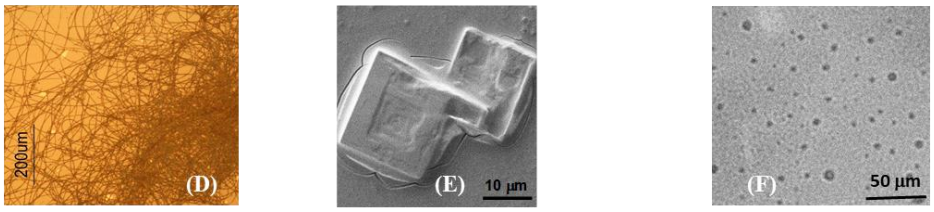

Chart 1. Organometallic precursors used in this work (**A**-**C**) and corresponding supramolecular assemblies of the aqueous dried samples observed under optical (D for **A**) and scanning electron microscopy (E and F for **B** and **C** respectively) in water.[28]

The use of catalytic amounts of Ag(0) for the reduction processes, together with the easy and well-established methodologies for the synthesis of the organometallic Au(I) starting molecules,[33] makes this method very promising since it is fast, clean and no side products must be eliminated in the reaction medium, since the organic material disappears by direct filtration.

The synthesis of the Au(0) microstructures was performed by modification of a methodology previously reported in the literature,[29] by the reaction of an aqueous solution of the organometallic complex with previously synthesized Ag NPs in a 200:1 molar ratio (Scheme 1).

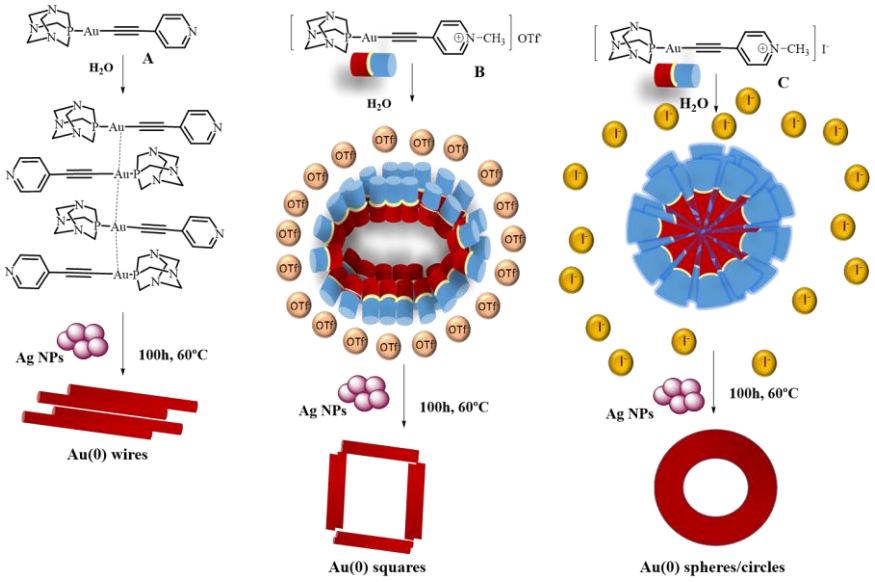

Scheme 1. General representation of the experimental procedure for the formation of Au(0) microstructures.

Different reaction conditions (temperature, time and solvent) were assayed to obtain the more homogeneous and reproducible resulting microstructures. 2 mL of a 20 mM aqueous solution of **A**-**C** (Chart 1) was stirred for 15 min at room temperature to form the supramolecular organometallic assemblies. Then, the solution was heated to 60ºC

and 2μL of 100 mM aqueous suspension of *ca*. 10 nm Ag NPs (Figure S1) were added and the reaction was maintained under stirring at 60ºC for 100 h. Under the reaction conditions the color of the mixture changed from pale yellow to dark orange (Figure S2). The resulting Au(0) nano- / microstructures were isolated after the addition of 2mL of acetone, sonication for 5 seconds and centrifugation for 5 min at 3900 rpm and analyzed by SEM.

Figures 1 and S3-S4 show representative SEM images of the Au(0) microstructures obtained by the reduction of the supramolecular organometallic structures together with the corresponding EDX analysis pattern of Au. As can be observed, the rod, square-based prism and spherical morphologies give rise to Au(0) materials with analogous shapes as a general trend after the reduction process that can be individually detected by this technique. The presence of solely Au in the EDX analysis (no Ag was detected in the microstructures) indicates that the structures were purely composed of this metal. The brightness detected in the backscattered detector based images (Figures S4 right) supports the presence of Au(0) in the structures.

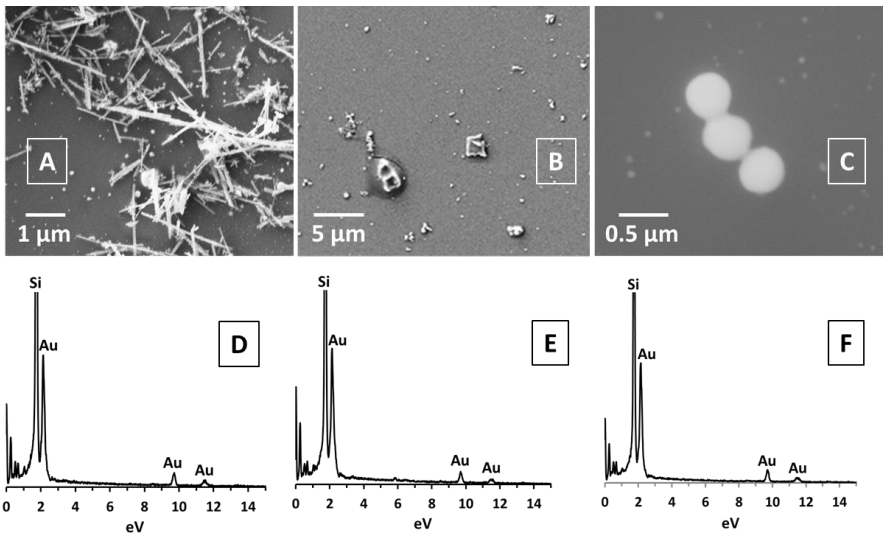

Figure 1. SEM images of the Au(0) structures obtained from the reduction of **A** (A); **B** (B) and **C** (C) and corresponding EDX analysis of **A** (D), **B** (E) and **C** (F).

Figure 1A shows that the reduction of the fibers formed by self-aggregation of the neutral compound A in water originates a rod morphology, which measure about 3 μm x 100 nm x 100 nm. This represents a decrease on the dimensions of the organometallic

fibers, which display sizes of up to few millimeters.[21] Figure 1B shows the formation of square-based prism Au microstructures (around 2 μm length and presumably 1 μm height) and Figure 1C shows spherical Au structures with an average diameter of 450 nm, both evidencing a significant shrinkage of the starting organometallic assemblies during reduction like in the case of the rods. This clearly demonstrates that the pre-organization of the starting self-assembled supramolecular organometallic structures (as fibers, squares or vesicles[28]) determines the resulting shape of the Au microstructures. This shape control merits to be highlighted and shows an easy and effective way to obtain different type of Au(0) microstructures by choosing the appropriate starting supramolecular assembly.

The analysis of the samples by TEM verifies the empty morphology of the samples, obtained through the reduction of the supramolecular aggregates, and evidences the nanoscale character of the material since microstructures are indeed formed by the controlled aggregation of spherical nanoparticles of 7 nm in average diameter.

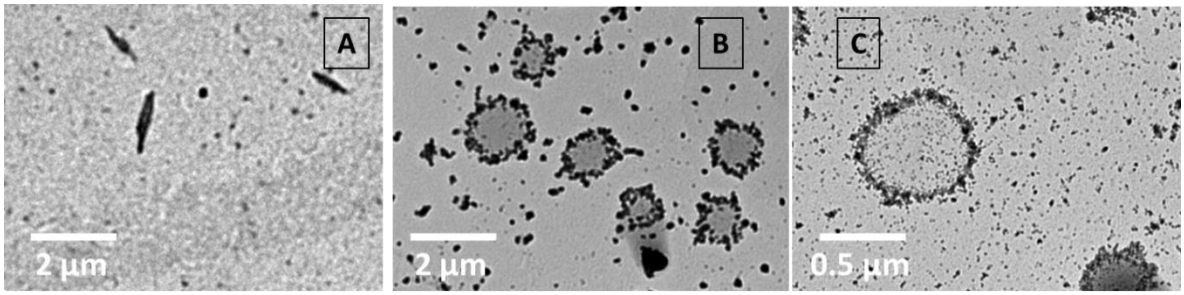

Figure 2. TEM images of the Au(0) structures obtained from the reduction of **A** (A); **B** (B) and **C** (C).

The aforementioned experiments were performed at a Au(I):Ag ratio of 200:1. We analyzed if this ratio could have a direct influence on the reaction being able to decrease the reaction time or temperature. However, at Au(I) : Ag ratios of 1:1 and 10:1, an undesired mixture of self-aggregated Au NPs, Ag NPs and organometallic precursor was determined by SEM-EDX to coexist in the samples (Figure S5).

These results suggest that the reduction reaction should be performed in catalytic conditions, being the ideal conditions Au(I) : Ag = 200:1 ratio to be able to complete the process and obtain homogeneous Au(0) microaggregates with shapes pre-determined by the supramolecular organometallic assemblies.

The presence of Au(0) in the resulting structures was identified in solution by recording the plasmon UV-visible band characteristic of this metal around 550 nm (Figure 3), which is similar to the recorded for Au(0) NPs previously synthesized in our group.[34] That is, the band corresponds to the plasmon of the individual Au(0) NPs that, as can be observed by TEM (Figure 2), are assembled in a specific way, defining the different shapes. At the same time and, as expected, the Ag(0) plasmon of the starting reagent (see Figure S6) disappeared. The broader bands in the UV-vis spectra of **A** and **C** could be due to the stronger interparticle interaction between single Au(0) NPs, compared to the **B**, with better-defined band in the UV-vis spectrum.[35] The absorption spectra were also collected in the near-infrared region for the three samples: no longitudinal plasmon band was observed in that region for any of the samples, confirming the spherical-like shape of the Au nanoparticles acting as building blocks in the formation of the observed superstructures.[1]

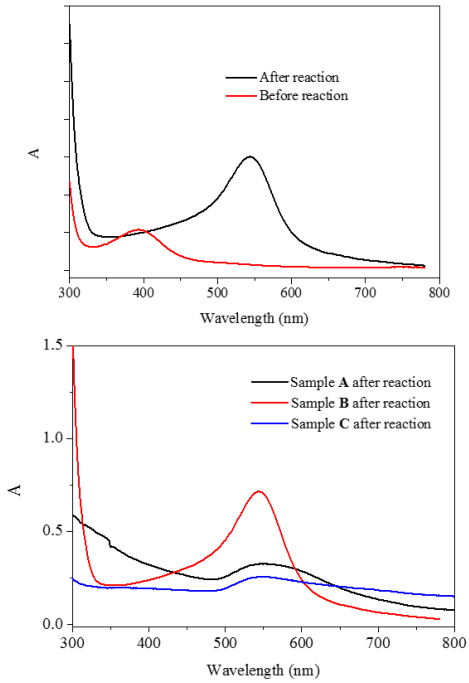

Figure 3. UV-visible spectra of an aqueous solution of **B** before (red line) and after (black line) reaction with Ag NPs (above); UV-visible spectra of aqueous solutions of **A**, **B** and **C** after reduction (below).

Taking into consideration that the solvent may also have a direct influence on the resulting supramolecular shapes or aggregates,[28] we have studied the morphology of the Au microstructures resulting from the reduction with Ag NPs of the **A** supramolecular assembly in chloroform and methanol instead of water. Star-like shapes are obtained

when chloroform is used. The stars are formed by the assembly of individual rods that share a common central point, originating this nice shape composed of Au (Figures 3 and S7) that can be formed due to different preorganization of the supramolecular assemblies in chloroform before the reduction process. Less homogeneous structures with a button-type shape were observed when the reaction is performed in methanol (Figure S8).

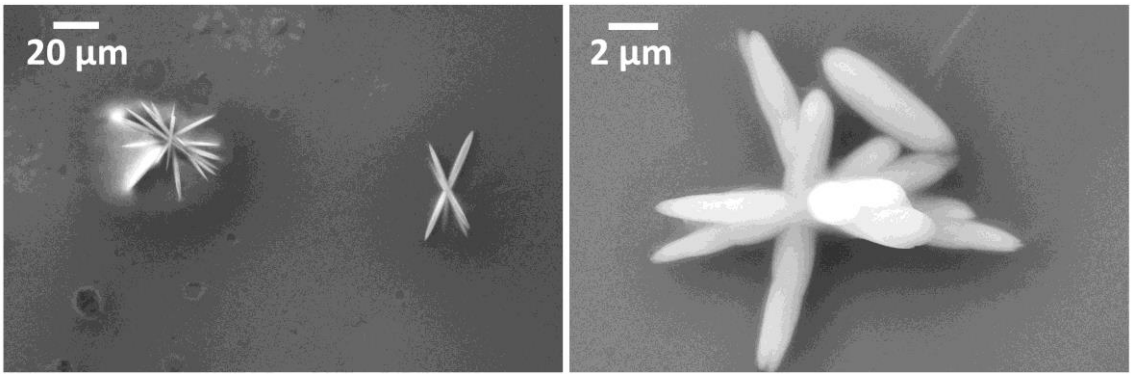

Figure 3. SEM characterization of the reaction of **A** with Ag NPs in 200:1 ratio in chloroform.

n view of the different morphologies of Au(0) microstructures displayed in this work, the formation of other Au(0) morphologies from Au(I) assemblies is envisioned. Here we have shown a high-yield fabrication of gold structures in a rational way upon the selective reduction of Au(I) organometallic supramolecular assemblies.

Conclusions

The formation of Au(0) microstructures with different morphologies is possible in an easy and controlled way upon reduction of well-defined supramolecular organometallic aggregates with Ag(0) nanoparticles. Remarkably, the original shape of the supramolecular organometallic aggregates is maintained in the Au(0) structures when the reaction is conducted in water. The choice of the solvent, temperature and Au(I):Ag(0) ratio are key points for the successful reaction. It has been observed that catalytic amounts of Ag(0) NPs are the best conditions for a neat reaction process. Additionally, different Au(0) morphologies can be obtained changing the polarity of the solvent.

Conflicts of interest

There are no conflicts to declare.

Acknowledgements

The authors are grateful to the Spanish Ministerio de Ciencia, Innovación y Universidades (AEI/FEDER, UE Project CTQ2016-76120-P). FCT/MCTES is acknowledged for financial support through the Associate Laboratory for Green Chemistry, LAQV-REQUIMTE (UID/QUI/50006/2013) and through Project PTDC/QUI-QFI/32007/2017. The authors also acknowledge financial support from the Spanish Ministerio de Economía y Competitividad (MINECO) through CTQ2015-68370-P. A.F. is a Serra Húnter fellow and acknowledges the regional Generalitat de Catalunya authority (2017 SGR 15). JL is a Serra Húnter Fellow and is grateful to ICREA Academia program and GC 2017 SGR 128. This research was also supported by a Marie Curie Intra European Fellowship within the 7th European Community Framework Programme (to R.G.).

References

1 T. K. Sau, A. L. Rogach, F. Jäckel, T. A. Klar and J. Feldmann, *Adv. Mater.*, 2010, **22**, 1805–1825.

2 J. Xiao and L. Qi, *Nanoscale*, 2011, **3**, 1383.

3 M. Dalmases, A. Pinto, P. Lippmann, I. Ott, L. Rodríguez and A. Figuerola, *Front. Chem.*, 2019, **7**, 1–10.

4 P. Li, H. Zhan, S. Tian, J. Wang, X. Wang, Z. Zhu, J. Dai, Y. Dai, Z. Wang, C. Zhang, X. Huang and W. Huang, *ACS Appl. Mater. Interfaces*, 2019, **11**, 13624–13631.

5 R. Takahata and T. Tsukuda, *Chem. Lett.*, 2019, **48**, 906–915.

6 R. A. Sperling, P. Rivera Gil, F. Zhang, M. Zanella and W. J. Parak, *Chem. Soc. Rev.*, 2008, **37**, 1896.

7 Z. Nie, D. Fava, E. Kumacheva, S. Zou, G. C. Walker and M. Rubinstein, *Nat. Mater.*, 2007, **6**, 609–614.

8 J. Xiao and L. Qi, *Nanoscale*, 2011, **3**, 1383.

9 H. Lv, D. Xu, J. Henzie, J. Feng, A. Lopes, Y. Yamauchi and B. Liu, *Chem. Sci.*, 2019, **10**, 6423–6430.

10 C. Zhu, D. Du, A. Eychmüller and Y. Lin, *Chem. Rev.*, 2015, **115**, 8896–8943.

11 Q. Zhang, S. Gupta, T. Emrick and T. P. Russell, *J. Am. Chem. Soc.*, 2006, **128**, 3898–3899.

12 M. A. Correa-Duarte, J. Pérez-Juste, A. Sánchez-Iglesias, M. Giersig and L. M. Liz-Marzán, *Angew. Chemie Int. Ed.*, 2005, **44**, 4375–4378.

13 J. George, S. Kar, E. S. Anupriya, S. M. Somasundaran, A. D. Das, C. Sissa, A. Painelli and K. G. Thomas, *ACS Nano*, 2019, **13**, 4392–4401.

14 L. Jin, B. Liu, M. E. Louis, G. Li and J. He, *ACS Appl. Mater. Interfaces*, 2020, acsami.9b20231.

15 J.C. Lima and L. Rodríguez, *Chem. Soc. Rev.*, 2011, **40**, 5442.

16 M. Pujadas and L. Rodríguez, *Coord. Chem. Rev.*, 2020, **408**, 213179.

17 J.C. Lima and L. Rodríguez, *Inorganics*, 2014, **3**, 1–18.

18 H. Cheng, S. Yan, J. Li, J. Wang, L. Wang, Z. Skeete, S. Shan and C. Zhong, *ACS Appl. Mater. Interfaces*, 2018, **10**, 40348–40357.

19 R. Ezquerra, S. G. Eaves, S. Bock, B. W. Skelton, F. Pérez-Murano, P. Cea, S. Martín and P. J. Low, *J. Mater. Chem. C*, 2019, **7**, 6630–6640.

20 E. Aguiló, A. J. Moro, R. Gavara, I. Alfonso, Y. Pérez, F. Zaccaria, C. F. Guerra, M. Malfois, C. Baucells, M. Ferrer, J. C. Lima and L. Rodríguez, *Inorg. Chem.*, 2018, **57**, 1017–1028.

21 E. Aguiló, R. Gavara, J.C. Lima, J. Llorca and L. Rodríguez, *J. Mater. Chem. C*, 2013, **1**, 5538.

22 R. Gavara, J. Llorca, J.C. Lima and L. Rodríguez, *Chem. Commun.*, 2013, **49**, 72–74.

23 R. Gavara, E. Aguiló, C. Fonseca Guerra, L. Rodríguez and J. C. Lima, *Inorg. Chem.*, 2015, **54**, 5195–5203.

24 A. J. Moro, B. Rome, E. Aguiló, J. Arcau, R. Puttreddy, K. Rissanen, J. C. Lima and L. Rodríguez, *Org. Biomol. Chem.*, 2015, **13**, 2026–2033.

25 A. Pinto, G. Hernández, R. Gavara, E. Aguiló, A. J. Moro, G. Aullón, M. Malfois, J. C. Lima and L. Rodríguez, *New J. Chem.*, 2019, **43**, 8279–8289.

26 R. Gavara, J.C. Lima and L. Rodríguez, *Photochem. Photobiol. Sci.*, 2016, **15**, 635–643.

27 A. Pinto, N. Svahn, J.C. Lima and L. Rodríguez, *Dalt. Trans.*, 2017, **46**, 11125–11139.

28 E. Aguiló, R. Gavara, C. Baucells, M. Guitart, J. C. Lima, J. Llorca and L. Rodríguez, *Dalt. Trans.*, 2016, **45**, 7328–7339.

29 X. Lu, M. S. Yavuz, H.-Y. Tuan, B. A. Korgel and Y. Xia, *J. Am. Chem. Soc.*, 2008, **130**, 8900–8901.

30 Y. Lu, S. Yang, J. Xu, Z. Liu, H. Wang, M. Lin, Y. Wang and H. Chen, *Small*, 2018, **14**, 1801925.

31 J. Cordón, G. Jiménez-Osés, J. M. López-de-Luzuriaga and M. Monge, *Nat. Commun.*, 2017, **8**, 1657.

32 Z. Wu, Y. Du, J. Liu, Q. Yao, T. Chen, Y. Cao, H. Zhang and J. Xie, *Angew. Chemie Int. Ed.*, 2019, **58**, 8139–8144.

33 M. Pujadas and L. Rodríguez, *Coord. Chem. Rev.*, 2020, **408**, 213179.

34 M. Dalmases, E. Aguiló, J. Llorca, L. Rodríguez and A. Figuerola, *ChemPhysChem*, 2016, **17**, 2190–2196.

35 S. K. Ghosh and T. Pal, *Chem. Rev.*, 2007, **107**, 4797–4862.